ISBN: 978-3-95450-227-1 ISSN: 2673-5490 doi:10.18429/JACoW-IPAC2022-TUPOST005

RF VOLTAGE CALIBRATION USING PHASE SPACE TOMOGRAPHY IN THE CERN SPS

D. Quartullo*, S. Albright, H. Damerau, A. Lasheen,
G. Papotti, C. Zisou, CERN, Geneva, Switzerland

Abstract

Voltage calibration using longitudinal phase-space tomography is a purely beam-based technique to determine the effective RF voltage experienced by a bunch. It was applied in the SPS, separately to each of its six accelerating travelling wave structures. A low spread in voltage errors was obtained by carefully optimizing the number of acquired bunch profiles. The technique moreover provided the relative phases of the cavities, which allowed their alignment to be checked. Pairs of cavities were measured as well to validate the consistency of the single-cavity voltages. The beam measurements were repeated after several months to confirm the reproducibility of the results. Longitudinal beam dynamics simulations, including the full SPS impedance model, were performed as a benchmark. The aim was to verify that the effect of the cable transfer-function on the bunch profiles can be neglected, as well as collective effects and small errors in the accelerator parameters.

INTRODUCTION

Longitudinal phase-space tomography is used to reconstruct the bunch distribution in longitudinal phase-space from a set of measured bunch profiles as input [1–5]. The discrepance D gives the average of the absolute differences between measured and reconstructed profiles. The discrepance usually decreases during the iterative reconstruction process and converges to an equilibrium value $\widehat{D}$ after a sufficient number of iterations.

The actual RF voltage V_d acting on the beam and the phase position $\widehat{\varphi}_\mathrm{s}$ of the bucket center with respect to the acquisition trigger are difficult to measure with conventional techniques. The voltage V_d can be considerably different from the programmed one V_p, due to the limited precision of electrical voltage measurements and collective effects.

Longitudinal tomography can be used to determine V_d and $\widehat{\varphi}_\mathrm{s}$ [6, 7]. One approach is to perform tomographic reconstructions for $(V_\mathrm{rf}, \varphi_\mathrm{s})$ pairs forming a rectangular grid, then the pair giving the minimum $\widehat{D}$ determines the actual V_d and $\widehat{\varphi}_\mathrm{s}$. An alternative method uses a minimization algorithm which creates a path converging to the minimum $\widehat{D}$ in the $(V_\mathrm{rf}, \varphi_\mathrm{s})$ parameter space (Fig. 1, middle).

In this paper, tomography-based voltage calibrations are applied to the SPS fundamental-harmonic RF system. Firstly, voltage-calibration results derived from measurements taken in 2021 are reported. Then, the consistency and reliability of the voltage errors are verified by examining the synchrotron oscillations of the measured profiles, by applying calibrations to multiple cavities, and by using simulated bunch-profile data as input for tomography. Finally, preliminary results from voltage calibrations done in 2022 are reported.

* danilo.quartullo@cern.ch

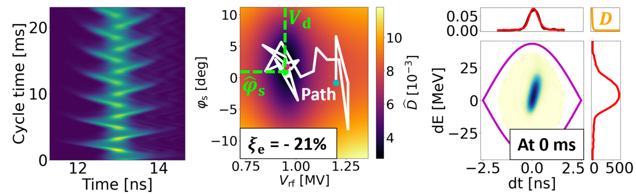

Figure 1: Left: example of bunch profiles measured in 2021 at SPS flat bottom. Only cavity 3 was active with V_p = 1.2 MV. Middle: corresponding voltage calibration. Right: phase-space reconstruction at injection. The measured (black) and reconstructed (red) bunch profiles overlap.

MEASUREMENTS SETUP

Beam measurements were performed at SPS injection energy during the first 23 ms (Fig. 1, left). A bunch with low intensity $N_\mathrm{p} < 5 \cdot 10^9$ p/b (protons per bunch) and smallest possible longitudinal emittance was generated by longitudinal shaving in the PSB and accelerated in the PS like a conventional single bunch for the LHC. The resulting bunch length at extraction from the PS was only about 1 ns.

Measurements were done in a single-harmonic RF system. Only one (or a subset) of the six accelerating RF cavities was active during a given cycle. Although the recorded bunch intensity was small, the Low Level RF (LLRF) One-Turn Delay Feedback (OTDFB) for beam-loading compensation was activated, since the set point of the OTDFB defines the voltage reference in the SPS [8].

Energy and phase mismatches between the PS and the SPS led to significant dipole oscillations (Fig. 1, left), which are crucial for tomography-based voltage calibrations. The beam-based LLRF loops were disabled to avoid damping dipole oscillations during measurements.

VOLTAGE CALIBRATIONS IN 2021

Two sets of measurements were taken in July and October. Five accelerator cycles were measured for each cavity to verify the reproducibility of results. The dependence of the relative voltage-error $\xi_\mathrm{e} = (V_\mathrm{d} - V_\mathrm{p})/V_\mathrm{p}$ on the number of synchrotron periods N_{T_s} used for voltage calibrations was investigated (Fig. 2). The measurement of ξ_e reached a convergence between 4 and 5 synchrotron periods, therefore only the voltage errors with $N_{T_\mathrm{s}} \in [4, 5]$ were considered.

Table 1 summarizes the voltage-calibration results. The average voltage errors vary between -21% and +3%, with spreads all within 1%. Comparing corresponding measure-

ISBN: 978-3-95450-227-1 ISSN: 2673-5490 doi:10.18429/JACoW-IPAC2022-TUPOST005

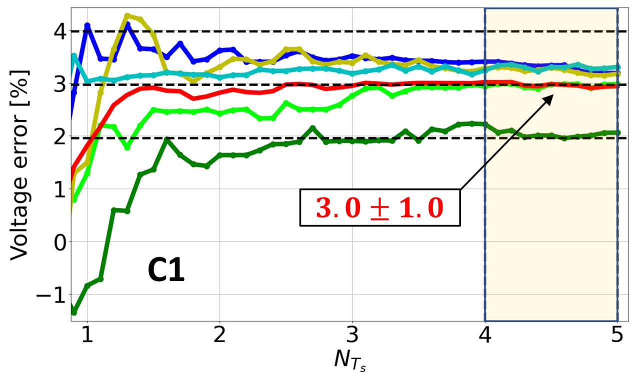

Figure 2: Voltage errors of cavity 1 as a function of the number of synchrotron periods considered for voltage calibrations, using as input the beam measurements taken in October 2021. The results of the five measured cycles are marked with a different color, the red line represents the average. The reported voltage-error average and spread are computed by considering only the data in the shaded area, where convergence is reached.

Table 1: Voltage calibration results for single cavities using measurements taken in July (first row) and October (second row). From left to right: cavity number, programmed voltage, average detected voltage, average voltage error with spread, average phase position of the bucket center with spread. The average phase positions are evaluated considering cavity 1 as reference.

C	V_p [MV]	$\langle V_\mathrm{d}\rangle$ [MV]	$\langle \xi_e \rangle \pm$ spread [%]	$\langle \widehat{\varphi}_\mathrm{s} \rangle \pm$ spread [deg]
1	0.9	0.927	3.0 ± 0.7	0 ± 0.3
		0.927	3.0 ± 1.0	0 ± 1.0
2	0.9	0.843	-6.3 ± 1.0	3.4 ± 0.6
		0.839	-6.8 ± 0.3	5.4 ± 0.5
3	1.2	0.956	-20.4 ± 0.7	0 ± 0.8
		0.950	-20.8 ± 0.4	0.6 ± 0.8
4	0.9	0.783	-13.0 ± 0.9	-0.2 ± 1.0
		0.784	-12.9 ± 0.2	-0.2 ± 0.6
5	0.9	0.753	-16.4 ± 0.8	0.3 ± 0.9
		0.749	-16.8 ± 0.7	1.0 ± 0.8
6	1.2	1.058	-11.8 ± 0.7	-3.3 ± 0.3
		1.076	-10.3 ± 0.2	-2.6 ± 0.6

ments taken in July and October, the largest difference in average ξ_e is just 1.5%. Cavities 2 and 6 have the largest phase error with respect to the vector sum of all the cavities. The spreads of the bucket-center phases are within 1 deg.

Voltage calibrations were also applied to pairs of cavities and to all the cavities together. The goal was to verify that the vector sum of multiple cavities was close to the sum of the individual cavity voltages. Table 2 shows the results, the differences between total detected voltages and sums of single-cavity voltages are below 1%.

Table 2: Voltage calibration results for multiple cavities. For each pair of cavities, results from measurements taken in July (first row) and October (second row) are reported. All the cavities together were measured only in October (last row). From left to right: measured cavities, total programmed voltage, total detected voltage, sum of the single-cavity detected voltages (taken from Table 1), relative difference between total and single-cavity sum detected voltages, phase position of the bucket center. Columns from 3 to 6 report values averaged over five cycles. The average phase positions are evaluated considering cavity 1 as reference.

C	V_p [MV]	$\langle V_\mathrm{d}\rangle$ [MV]	$\Sigma\langle V_\mathrm{d}\rangle$ [MV]	$\langle V_\mathrm{d}\rangle - \Sigma\langle V_\mathrm{d}\rangle$ [%]	$\langle \widehat{\varphi}_\mathrm{s} \rangle$ [deg]
1,2	1.8	1.771	1.770	0.1	1.7
		1.766	1.766	0.0	3.1
3,6	2.4	2.020	2.014	0.3	−1.1
		2.029	2.026	0.1	−0.9
4,5	1.8	1.546	1.536	0.6	0.4
		1.537	1.533	0.3	1.1
All	6.0	5.333	5.325	0.2	1.5

CONSISTENCY CHECKS USING SYNCHROTRON FREQUENCY RATIOS

To confirm that single-cavity voltage errors were consistent with respect to each other, small-amplitude synchrotron frequency $f_{\mathrm{s},0}$ ratios were computed as either square roots of detected-voltage ratios or as ratios of synchrotron periods. Detected voltages were derived from voltage calibrations, whereas the synchrotron periods were evaluated by examining the evolution of dipole bunch oscillations.

As an example, Fig. 3 compares cycles measured with either cavity 1 or 5. The average synchrotron periods are 3.46 ms and 3.87 ms for cavities 1 and 5, respectively. The ratio of synchrotron periods is 1.12, whereas the $f_{\mathrm{s},0}$ ratio using average detected-voltages (Table 1) is 1.11. Thus, the two methods agree within 1%, indicating that the voltage errors are consistent amongst each other.

BENCHMARKS WITH SIMULATED DATA

To benchmark the tomography-based voltage calibration method and study potential systematic errors, realistic macroparticle simulations were performed with the CERN BLonD code [9] and the simulated profiles (Fig. 4, top right) were used as input for the analysis.

To compare with measurements, the simulated initial distribution had $N_\mathrm{p} = 5 \cdot 10^9$ p/b and a bunch length of 1 ns. The assumed RF voltage was 0.9 MV. The full SPS longitudinal impedance model and space charge [10] were added in simulations (Fig. 4, top left), but the effect of the OTDFB was not included. The transfer function of the cables connecting the longitudinal pick-ups to the acquisition system was applied to the simulated profiles, making them more similar to the measured ones.

ISBN: 978-3-95450-227-1 ISSN: 2673-5490 doi:10.18429/JACoW-IPAC2022-TUPOST005

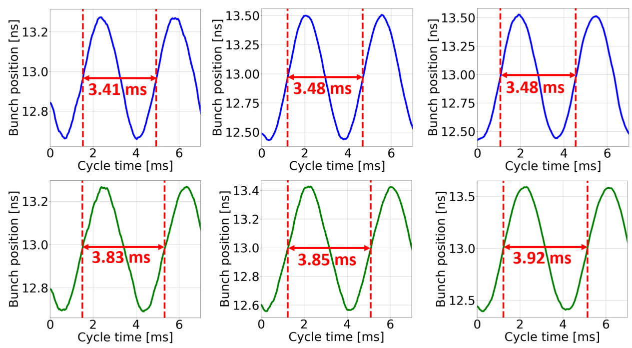

Figure 3: Bunch-position evolutions for cycles measured with only cavity 1 (top) or cavity 5 (bottom), the programmed voltage is 0.9 MV. The bunch positions are the middle points of the profiles FWHM. For each plot, the vertical lines determine one synchrotron period.

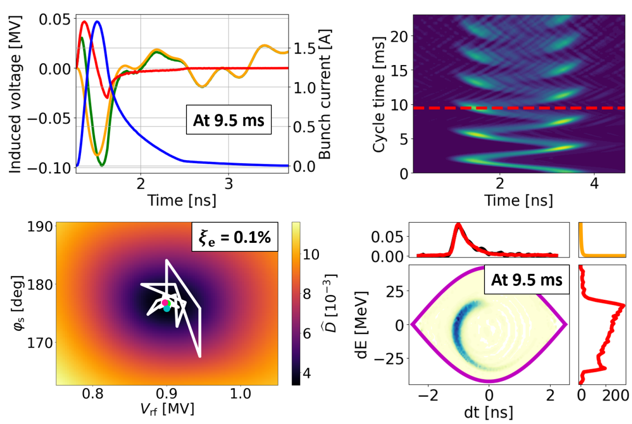

Figure 4: Top left: example of simulated profile (blue) with space-charge (red), impedance (orange) and total (green) induced voltages. Top right: simulated profiles used for voltage calibration. The red line marks the cycle time 9.5 ms. Bottom left: outcome of the voltage calibration. Bottom right: phase-space reconstruction at 9.5 ms.

The tomographic reconstructions needed for the voltage calibration were performed without including collective effects, as done for the calibrations with measured data. The assumed RF voltage was reproduced with an error of just 0.1% (Fig. 4, bottom left). Then, using the same simulated profiles, the voltage calibration was repeated introducing an error of 1% in the design momentum. The obtained ξ_e was just 0.4%. This validated the voltage-calibration method and also indicated that the effect of the cable transfer-function on the profiles can be neglected, as well as collective effects and small inaccuracies in the accelerator parameters.

PRELIMINARY VOLTAGE CALIBRATIONS IN 2022

More accurate electrical gap-voltage calibrations for all the SPS cavities were performed in January 2022. A new set of beam measurements was taken and tomography-based voltage calibrations were performed.

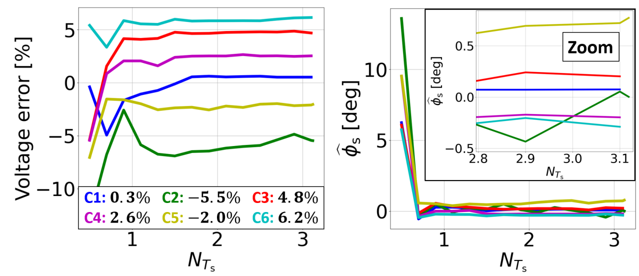

Figure 5: Voltage errors (left) and phase positions of the bucket centers (right) as a function of the number of synchrotron periods used for voltage calibrations. The measurements were taken in early 2022 (only one cycle per cavity). The programmed voltage was 1.37 MV (4 sections) for cavities 3 and 6, 0.86 MV (3 sections) for the other cavities. The voltage errors at $N_{T_s} = 3$ are reported in the legend.

As Fig. 5 shows, the voltage errors were improved compared to those found in 2021. The phase alignments between cavities were better in 2022, with a maximum misalignment of only 1 deg. The sum of the six programmed voltages (6.16 MV) differs from the sum of single-cavity detected voltages (6.27 MV) by less than 2%. This confirms that the electrical voltage calibrations were successful.

CONCLUSIONS

Voltage calibration using longitudinal tomography was applied to the SPS accelerating RF cavities. First measurements in 2021 indicated voltage errors up to 21% and showed a good phase alignment between cavities, except for cavities 2 and 6. Two sets of measurements taken in July and October provided very similar results.

Voltage calibrations for multiple cavities were also performed. The disagreements between total detected voltages and sums of single-cavity voltages were below 1%. This validated the voltage error found for each cavity. Estimates of synchrotron-frequency ratios using either detected voltages or synchrotron periods indicated that the voltage errors of the six cavities were consistent with respect to each other.

Realistic macro-particle simulations were performed and the simulated profiles were used as input for voltage calibration. The voltage errors were below 1%, showing that the results obtained with the measured profiles can be trusted.

Tomography-based voltage calibrations were repeated in early 2022 after the realization of more accurate electrical RF voltage measurements. Voltage errors were significantly lower than the ones found in 2021, all the cavities were aligned within 1 deg, and the difference between the sum of programmed voltages and the sum of single-cavity detected voltages was less than 2%. This confirmed the success of the electrical measurement campaign.

ACKNOWLEDGMENTS

We thank our colleagues Philippe Baudrenghien and Gregoire Hagmann for having performed and refined electrical voltage calibrations for the SPS RF cavities in January 2022.

ISBN: 978-3-95450-227-1 ISSN: 2673-5490 doi:10.18429/JACoW-IPAC2022-TUPOST005

REFERENCES

[1] S. Hancock, M. Lindroos, and S. R. Koscielniak, "Longitudinal phase space tomography with space charge," *Phys. Rev. ST Accel. Beams*, vol. 3, p. 124 202, 2000, doi:10.1103/PhysRevSTAB.3.124202

[2] S. Hancock, P. Knaus, and M. Lindroos, "Tomographic measurements of longitudinal phase space density," Tech. Rep. CERN, Geneva, Switzerland, CERN-PS-98-030-RF, 1998.

[3] S. Hancock, "Tomography at injection in the PSB," Tech. Rep. CCERN, Geneva, Switzerland, ERN-ACC-NOTE-2016-0040, 2016.

[4] C. H. Grindheim and S. Albright, "Longitudinal phase space tomography version 3," Tech. Rep. CERN-ACC-NOTE-2021-0004, Geneva, Switzerland, 2021.

[5] S. Albright, "A proposal for an automatic longitudinal tomography demonstration project in the Proton Synchrotron Booster," Tech. Rep. CERN, Geneva, Switzerland, CERN-ACC-NOTE-2020-0014, 2020.

[6] S. Hancock, M. Angoletta, and A. Findlay, "LEIR RF voltage calibration using phase space tomography," Tech. Rep. CERN, Geneva, Switzerland, CERN-ATS-Note-2010-055 MD, 2010.

[7] D. Quartullo, S. Albright, and H. Damerau, "Frequency-dependent RF voltage calibration using longitudinal tomography in the CERN PSB," in *Proc. of International Particle Accelerator Conference (IPAC'22)*, Bangkok, Thailand, 2022, this conference.

[8] F. J. Galindo Guarch, P. Baudrenghien, and J. M. Moreno Arostegui, "A new beam synchronous processing architecture with a fixed frequency processing clock. Application to transient beam loading compensation in the CERN SPS machine," *Nuclear Instruments and Methods in Physics Research Section A: Accelerators, Spectrometers, Detectors and Associated Equipment*, vol. 988, p. 164 894, 2021.

[9] CERN Beam Longitudinal Dynamics code BLonD, http://blond.web.cern.ch/.

[10] J. Repond, "Possible Mitigations of Longitudinal Intensity Limitations for HL-LHC Beam in the CERN SPS," Ph.D. dissertation, Lausanne EPFL and CERN, 2019, https://cds.cern.ch/record/2695204